ACI STRUCTURAL JOURNAL TECHNICAL PAPER

Title no. 106-S20

Deformation Capacity of Reinforced Concrete Columns

by Hossein Mostafaei, Frank J. Vecchio, and Toshimi Kabeyasawa

An effective approach is presented for estimation of the ultimate deformation and load capacity of reinforced concrete columns based on principles of axial-shear-flexure interaction. Conventional section analysis techniques are employed for modeling the flexure mechanism, and the simplified modified compression field theory is implemented for modeling the shear behavior of elements. Average centroidal strains and average concrete compression strains derived from the flexural model are implemented in the shear model and used to calculate shear deformation and concrete strength degradation. This approximate procedure can be easily implemented in a hand-calculation method in a few steps. The approach is employed for the estimation of the ultimate deformation of shear- and flexure-dominated reinforced concrete columns previously tested. The analytical results are compared with the experimental data and consistent, strong agreement is achieved.

Keywords: axial deformation; axial-shear-flexure interaction; displacement-based evaluation; ductility; ultimate deformation; ultimate strength.

INTRODUCTION

Although the behavior of reinforced concrete columns and beams has been studied for more than 100 years, the problem of estimating ultimate deformation at ultimate strength, or the lateral deformation at shear failure, remains unsolved. Experimental studies by various authors[1,2] revealed that reinforced concrete columns subjected to axial load and lateral load with similar ultimate strength may fail in significantly different ultimate deformations. Although it is agreed that increasing the ratio of the transverse reinforcement will enhance the ductility of a column, determining the ultimate deformation at which the element fails in shear is still a major challenge for engineers. Based on newly introduced performance-based design philosophies for response estimation of structures, one of the main performance properties in the design process is the ductility and deformability of the structure. The more ductility the structure possesses, the better the performance and the more economical the design. Therefore, it is essential to have and apply a suitable analytical tool to accurately estimate the ultimate deformation or ductility of reinforced concrete column elements.

Recently, an attempt was made to include the effects of shear deformations in sectional analyses through the axial-shear-flexure interaction (ASFI) method.[3,4] The ASFI method was developed to improve not only the response simulation of reinforced concrete elements with dominant shear behavior, but also to improve the flexural response calculation capabilities of the fiber model approach. This was done by satisfying compatibility and equilibrium conditions for both the flexure and shear mechanisms employed in the ASFI method. In the approach, the flexure mechanism was modeled by applying traditional section analysis techniques, and shear behavior was modeled based on the modified compression field theory (MCFT).[5] The approach was implemented and verified for a number of reinforced concrete columns tested with different axial loads, transverse reinforcement ratios, longitudinal reinforcement ratios, and scales ranging from one-third to full-scale specimens. The application of the MCFT as a shear model within the ASFI method, however, requires relatively intensive computation—a calculation process involving inversion of a 3 x 3 matrix, and an iteration process converging five different variables, which might not be suited to engineers in practice. In addition, the results of analyses by the ASFI approach suggested further studies on the onset of shear failure or ultimate deformation of reinforced concrete columns.

Considering the fact that columns with either dominant flexure or shear response fail finally in shear, the main objective of this study was to provide a simple analytical model, applicable for design in practice, for determining the critical conditions that result in the shear failure of reinforced concrete columns and the corresponding ultimate strength and deformation capacity. In this new analytical process, tension-shear failure across cracks, loss of concrete compression strength, and compression-shear failure were the main failure mechanisms considered at the ultimate state for both shear- and flexure-dominant members. In addition, crushing of cover concrete, bond failure, buckling of compression bars, and rupture of reinforcement were other potential failure conditions and were checked at the ultimate state.

RESEARCH SIGNIFICANCE

Accurate estimation of the ultimate deformation and ductility of reinforced concrete elements has long been a significant challenge and the aim of researchers. A new approach was developed to estimate both the ultimate deformation and load capacity of reinforced concrete columns and beams. The proposed method can be used as an effective analytical tool for the purpose of displacement- and performance-based design.

ASFI METHOD AND UNIAXIAL SHEAR-FLEXURE MODEL

The ASFI method is composed of two models: a flexure model based on traditional uniaxial section analysis principles, and a shear model based on a biaxial shear element approach. The total lateral drift of a column between two sections, γ, is the sum of shear strain γ_s and the flexural drift ratio γ_f between the two sections. Furthermore, the total axial strain of the column between the two sections, ε_x, is the sum of axial strains due to axial ε_{xa}, shear ε_{xs}, and flexural ε_{xf}, (Fig. 1), mechanisms

$$\gamma = \gamma_s + \gamma_f \quad (1)$$

ACI Structural Journal, V. 106, No. 2, March-April 2009.
MS No. S-2007-281 received August 2, 2007, and reviewed under Institute publication policies. Pertinent discussion including author's closure, if any, will be published in the January-February 2010 *ACI Structural Journal* if the discussion is received by September 1, 2009.

Hossein Mostafaei *is a Postdoctoral Fellow in the Department of Civil Engineering at the University of Toronto, Toronto, ON, Canada. He received his PhD in structural/earthquake engineering from the University of Tokyo, Tokyo, Japan, in 2006. His research interests include displacement-based methodology, analytical and numerical modeling of reinforced concrete elements, seismic performance assessment, and rehabilitation of reinforced concrete structures.*

Frank J. Vecchio, *FACI, is a Professor in the Department of Civil Engineering at the University of Toronto. He is a member of Joint ACI-ASCE Committees 441, Reinforced Concrete Columns, and 447, Finite Element Analysis of Reinforced Concrete Structures. His research interests include nonlinear analysis and design of reinforced concrete structures; constitutive modeling; and assessment, repair, and rehabilitation of structures.*

Toshimi Kabeyasawa *is a Professor at the Earthquake Research Institute, University of Tokyo. His research interests include reinforced concrete structures, seismic performance evaluation, retrofit of existing structures, and structural dynamics.*

$$\varepsilon_x = \varepsilon_{xa} + \varepsilon_{xs} + \varepsilon_{xf} \quad (2)$$

The centroidal axial strain ε_{xc} is derived from a section analysis or axial-flexure model, and is defined as the sum of the strains due to axial and flexural mechanisms, $\varepsilon_{xc} = \varepsilon_{xaf} + \varepsilon_{xf}$. On the other hand, from the shear model for axial-shear elements, the sum of the axial strains due to axial and shear mechanisms is determined, $\varepsilon_s = \varepsilon_{xas} + \varepsilon_{xs}$. As a result, to obtain ε_x in Eq. (2), ε_{xf} must be extracted from ε_{xc} and added to ε_s, considering $\varepsilon_{xa} = \varepsilon_{xaf} = \varepsilon_{xas}$.

Equilibrium of the shear and axial stresses from the axial-flexure model, τ_f and σ_{xf}, and from the axial-shear model, τ_s and σ_{xs}, respectively, must be satisfied simultaneously through the analysis. That is

$$\sigma_{xf} = \sigma_{xs} = \sigma_o \quad (3)$$

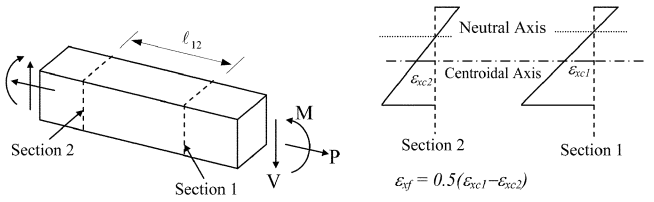

Fig. 1—Average centroidal strain due to flexure.

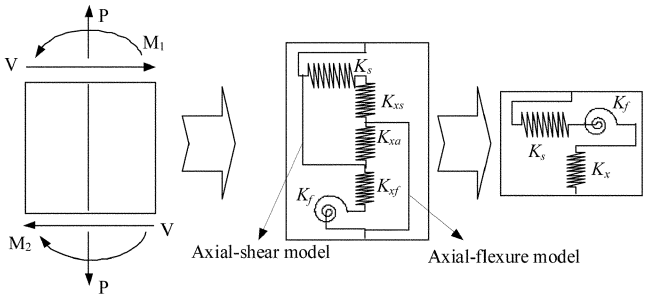

Fig. 2—Spring model of ASFI method.

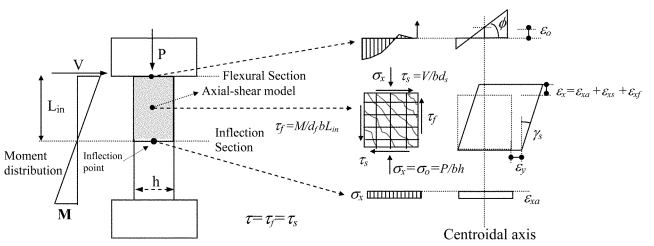

Fig. 3—Axial-shear-flexure interactions in ASFI method.

$$\tau_f = \tau_s = \tau \quad (4)$$

where σ_{xf} is the axial stress in the axial-flexure mechanism, σ_{xs} is the axial stress in the axial-shear mechanism, σ_o is the applied axial stress, τ_f is the shear stress in the axial-flexure mechanism, τ_s is the shear stress in the axial-shear mechanism, and τ is the applied shear stress. Stresses in axes perpendicular to the axial axis of the column, the clamping stresses σ_y and σ_z are ignored due to equilibrium between confinement pressure and hoop stresses.

$$\sigma_y = \sigma_z = 0 \quad (5)$$

Figure 2 illustrates the two models for axial-shear and axial-flexure and their interactions by means of springs in series. Figure 3 illustrates the ASFI method for a reinforced concrete column with two end sections, including the equilibrium and compatibility conditions. The total axial deformations considered in the ASFI method were axial strains developed by axial, shear, and flexural actions, and by pullout mechanism.

In a uniaxial shear-flexural model applied in this study, compatibility was also satisfied for average concrete compression strains. Consider a reinforced concrete column of moderate height, fixed against rotation and translation at the bottom and free at the top, subjected to in-plane lateral load and axial load, as shown in Fig. 4. Given its pattern along the column (refer to Fig. 4(a)), the concrete principal compression strain for an element between two sections, ε_2, may be determined based on average values of the concrete uniaxial compression strains corresponding to the resultant forces of the concrete stress blocks.

$$\varepsilon_2 = 0.5(\varepsilon_{2_i} + \varepsilon_{2_{i+1}}) \quad (6)$$

This is the main hypothesis of the new method proposed herein; this assumption simplifies the shear model significantly from a biaxial to a uniaxial mechanism. For the column in

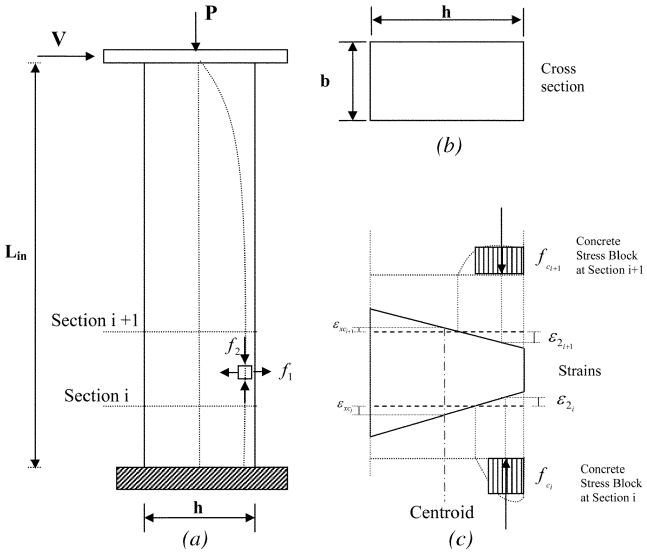

Fig. 4—A reinforced concrete column subjected to shear and axial loads: (a) concrete principal compression stress pattern; (b) cross section; and (c) stress blocks and strains at two adjacent sections.

Fig. 4, the compression strain obtained from Eq. (6) is set equal to the average principal compression strain of the element between the two sections of i and $i + 1$.

MODIFIED COMPRESSION FIELD THEORY

The shear mechanism in the ASFI method, as well as in this analytical process, was modeled according to the MCFT.[5] It is a suitable displacement-based evaluation approach for predicting the load-deformation response of reinforced concrete membrane elements subjected to shear and normal stresses. The MCFT is essentially a smeared rotating crack model. It includes compression softening effects, tension stiffening effects, and consideration of local conditions at cracks. The MCFT is based on orientations of the principal average strains in an element leading to the calculation of principal average stresses in concrete through concrete constitutive relationships. Transforming the average concrete principal stresses to the global coordinate axes and adding to the average stresses in the reinforcement gives the total average stresses in the element. There are two checks in the calculation process relating to the crack zones. The first is to ensure that tension in the concrete can be transferred across the crack. The second is to ensure that the shear stress on the surface of the crack does not exceed the maximum shear resistance provided by aggregate interlock. A reinforced concrete element within the context of the MCFT can be illustrated by the free body diagram of the membrane element depicted in Fig. 5.

DERIVATION OF ANALYTICAL MODEL

Considering the free body diagram of the membrane element in Fig. 6, equilibrium conditions in the MCFT require that

$$\sigma_x = f_{cx} + \sigma_{sx} f_{sx} \tag{7}$$

$$\sigma_y = f_{cy} + \sigma_{sy} f_{sy} \tag{8}$$

where, for beams and columns, σ_x is the total normal stress in the x-direction (that is, the applied axial stress); σ_y is the total normal or clamping stress in the y-direction, taken to be zero; f_{cx} and f_{cy} are stresses in concrete in the x (axial) and y (transverse) directions, respectively; ρ_{sx} and ρ_{sy} are the reinforcement ratios in the x (axial) and y (transverse) directions, respectively; and f_{sx} and f_{sy} are the stresses in the main bars (axial direction) and in the transverse reinforcement (y-direction), respectively.

A Mohr's circle for concrete stress yielded the following equilibrium relationships

$$f_{cx} = f_{c1} - \tau_s \cot\theta_c \tag{9}$$

$$f_{cy} = f_{c1} - \tau_s \tan\theta_c \tag{10}$$

$$f_{c2} = f_{c1} - \tau_s(\tan\theta_c + 1/\tan\theta_c) \tag{11}$$

where f_{c1} is the concrete principal tensile stress, f_{c2} is the concrete principal compressive stress, τ_s is the concrete shear stress, and θ_c is the crack angle.

On the other hand, the compatibility equation based on the Mohr's circle for strain requires that

$$\tan^2\theta_c = \frac{\varepsilon_x - \varepsilon_2}{\varepsilon_y - \varepsilon_2} \tag{12}$$

$$\varepsilon_1 + \varepsilon_2 = \varepsilon_x + \varepsilon_y \tag{13}$$

where ε_x is the axial strain, ε_y is the strain in the transverse reinforcement, ε_1 is the concrete principal tensile strain, and ε_2 is the concrete principal compression strain.

With ε_x obtained from section analysis, combining Eq. (9), (10), (12), and (13) yielded two useful equations for estimation of ε_y and ε_1.

$$\varepsilon_y = \sqrt{b^2 + c} - b \qquad \varepsilon_y < \varepsilon_{yy} \tag{14}$$

where ε_{yy} is the yield strain, and

$$b = \frac{f_{c1}}{2\rho_{sy}E_s} - \frac{\varepsilon_2}{2}, \qquad c = \frac{(\varepsilon_x - \varepsilon_2)(f_{c1} - f_{cx}) + f_{c1}\varepsilon_2}{\rho_{sy}E_s}$$

where E_s is the modulus of elasticity of transverse reinforcement. When strain in the transverse reinforcement is greater than the yield strain ε_{yy}, Eq. (15) can be applied

$$\varepsilon_1 = \frac{(\varepsilon_x - \varepsilon_2)(f_{c1} - f_{cx})}{(f_{c1} + \rho_{sy} f_{syy})} + \varepsilon_x \quad \varepsilon_y \geq \varepsilon_{yy} \tag{15}$$

where f_{syy} is the yield stress of transverse reinforcement and f_{cx} is determined based on Eq. (7). At the ultimate states, Eq. (15) is usually the governing equation. Given β as the concrete compression softening factor, an average initial value of $f_{c1} = 0.44 f_t'$ can be considered for Eq. (14) and (15)

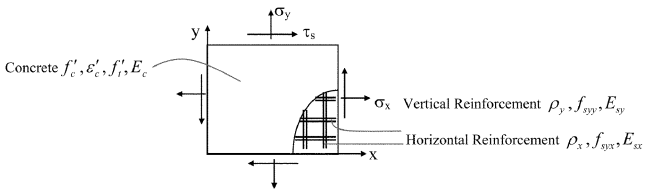

Fig. 5—A reinforced concrete membrane element subject to in-plane stresses.

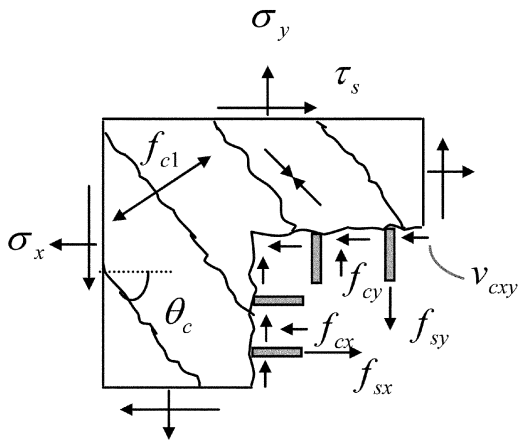

Fig. 6—Reinforced concrete in-plane shear element showing average stresses.

by assuming a tension stiffening model and an average tensile strain ε_1 that can be derived from Eq. (16) based on an upper bound of $\beta \le 1$ and lower bound of $\beta \ge 0.2$.

$$\beta = \frac{1}{0.8 - 0.34\dfrac{\varepsilon_1}{\varepsilon_c'}} \le 1.0 \quad (16)$$

where ε_c' is the concrete peak strain. The MCFT limits the shear stress transferred by aggregate interlock across a crack surface, τ_i, to the value given by Walraven's equation

$$\tau_i \le \frac{0.18\sqrt{f_c'}}{0.31 + \dfrac{24w}{a_g + 16}} \text{ (MPa, mm)} \quad (17)$$

where $w = s_\theta \varepsilon_1$, and $s_\theta = 1/[(\sin\theta_c/s_x) + (\cos\theta_c/s_y)]$, where s_x and s_y are the average crack spacings in the x- and y-directions, respectively, and a_g is the maximum aggregate size.

Equilibrium in the y-direction at the crack requires that

$$f_{sycr} = (\sigma_y + \tau_s \tan\theta_c - \tau_i \tan\theta_c)/\rho_{sy} \quad (18)$$

where f_{sycr} is the transverse reinforcement stress at the crack, and σ_y is the clamping stress, which is equal to zero. Hence, for $f_{sycr} = f_{syy}$, Eq. (18) yields

$$\tau_{max} \le \tau_i + f_{syy}\rho_{sy}\cot\theta_c \quad (19)$$

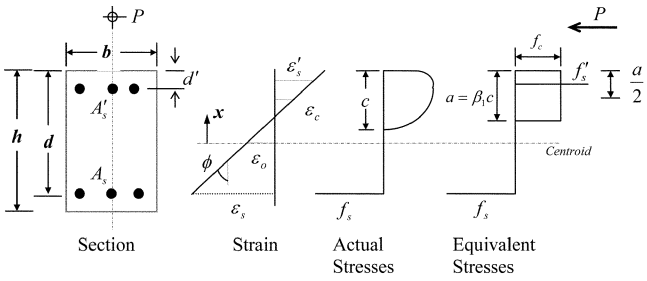

Fig. 7—Stresses and strains relations at critical flexural section, for example, bottom end-section in Fig. 4.

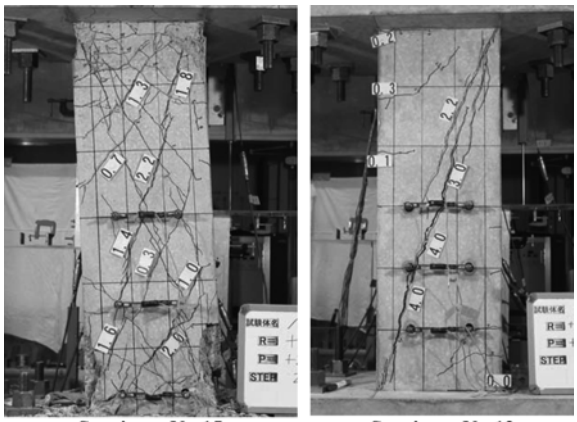

Fig. 8—Shear failure at ultimate deformation for both shear- and flexure-dominated columns.

FLEXURE MECHANISM

The traditional section analysis method is a handy and convenient approach for the evaluation of the flexural performance of a reinforced concrete column or beam. Because the analysis is implemented assuming a uniaxial stress field, material modeling and analytical computation are simple and a solution can be achieved with adequate convergence in a few steps. Figure 7 shows a flexural section for a column. The force-strain relationship for a section under uniaxial bending can be derived from axial load equilibrium as follows

$$\varepsilon_o \sum E_i A_i + \phi \sum E_i A_i x_i = P \quad (20)$$

where P is the applied axial load. Other components are

$$\sum E_i A_i = A_s E_s + A_s' E_s' + abE_c \quad (21a)$$

$$\sum E_i A_i X_i = A_s E_s 0.5(d - d') + A_s' E_s' 0.5(d' - d) + abE_c 0.5(a - h) \quad (21b)$$

where $E_s = f_s/\varepsilon_s$, $E_s' = f_s'/\varepsilon_s'$, $E_c = f_c/\varepsilon_c$, and $a = \beta_1 c$, and where β_1 is the rectangular stress block coefficient that is equal to 0.85 for $f_c' < 28$ MPa (4061 psi); β_1 is reduced continuously by 0.05 for each 7 MPa (1015.3 psi) above 28 MPa (1061 psi). The main assumption of plane sections yields the following relationships

$$\phi = \frac{-\varepsilon_c}{c(1 - 0.5\beta_1)} = \frac{\varepsilon_o}{0.5h - c} = \frac{-\varepsilon_s'}{c - d'} = \frac{\varepsilon_s}{d - c} \quad (22)$$

Solving Eq. (20) for ε_o and $\beta_1 = 0.85$ gives

$$\varepsilon_o = \frac{hP - 1.7391h[A_s'E_s' + A_sE_s + abE_c]\varepsilon_c}{2[d'A_s'E_s' + dA_sE_s + 0.5bE_ca^2]} + 1.7391\varepsilon_c \quad (23)$$

By determining f_s', f_s, and f_c, the bending moment within the section is obtained by applying moment equilibrium for the section

$$M = 0.5(d' - d)A_s'f_s' + 0.5(d - d')A_sf_s + 0.5(a - h)baf_c \quad (24)$$

If M is the end-moment of a column, as in Fig. 3, then flexural shear stress τ_f is determined based on Eq. (25)

$$\tau_f = \frac{M}{bd_fL_{in}} \quad (25)$$

where $d \le d_f \le h$ is assumed based on the failure mode described in the following.

PROCEDURES FOR ESTIMATION OF ULTIMATE DEFORMATION

The main failure mechanism for both shear- and flexure-dominated beams and columns is shear failure. Figure 8 shows Specimens 12 and 15 from Table 1 with shear and flexure responses, respectively; however, both failed in shear at the ultimate deformation. Bond failure, buckling of

compression bars, rupture of the tensile bars, and crushing of cover concrete are other failure criteria for reinforced concrete columns and beams. The analytical procedure presented herein is based on assuming shear failure as the main failure mechanism, and checking for the other failure criteria.

Three shear failure conditions are defined based on the MCFT as shear failure at a crack (Failure Mode 1), failure due to loss of compression strength (Failure Mode 2), and shear-compression failure (Failure Mode 3). Shear failure at a crack, which is typically the governing case for columns with low transverse reinforcement ratios, is determined using Eq. (19) and (25). Shear failure occurs when

$$\tau_f = \frac{M}{bd_f L_{in}} \geq \tau_i + f_{syy}\rho_{sy}\cot\theta_c \quad (26)$$

where $d_f = d$. Columns under high shear force, such as short columns, if not failing via Mode 1, will lose compression strength f_2 due to shear deformation and fail before the peak, $\varepsilon_2 \leq \varepsilon_c'$. This failure condition, Mode 2, is defined by Eq. (11) and (25) when

$$\tau_f = \frac{M}{bd_f L_{in}} \geq \frac{(f_{c1} - f_{c2})}{(\tan\theta_c + 1/\tan\theta_c)} \quad (27)$$

where $d_f = h$ for short columns with span-depth ratios less than 1.0 and $d_f = d$ for columns with span-depth ratios more than 1.5; for ratios between 1.0 and 1.5, d_f is determined by interpolation.

Columns and beams with a ductile flexure performance, when having sufficient transverse reinforcement and relatively low shear stress, will fail in shear when $\varepsilon_2 = \varepsilon_c'$ via Mode 3.

$$\tau_f = \frac{M}{bd_f L_{in}} \quad (28)$$

where $\varepsilon_2 = \varepsilon_2'$ and $d_f = h$. Finally, for flexure beams and columns with very low shear stress, especially under heavy cyclic loadings, the compression softening factor may be limited to $\beta \geq 0.15$. In other words, if β reduces to 0.15, then that will signal the ultimate state. None of the columns in Table 1 reached this limit within the range $\varepsilon_2 \leq \varepsilon_c'$, hence further study is required in regard to this condition.

Based on the shear failure criteria described previously, an analytical procedure can be constructed for the estimation of the ultimate deformation of a reinforced concrete column with a flexure section at the section with maximum moment, such as the column shown in Fig. 3. In step-by-step fashion, the procedure is as follows:

1. Assume an initial value for concrete compression strain of the flexure section, ε_c; for example, $\varepsilon_c = \varepsilon_c'$;
2. Employ Eq. (21) through (23) to determine the centroidal strain of the section, ε_o, through one or two iterations. Assume an initial value for ε_o; for example, $\varepsilon_o = 0.001$;
3. Determine the axial strain at the inflection point with zero moment, ε_{xa}, using basic sectional analysis principles;
4. Compute the average concrete principal compression strain ε_2 and axial strain ε_x for the shear model

Table 1—Material properties of test specimens

Specimen	Type	b, mm (in.)	h, mm (in.)	$2L_{in}$, mm (in.)	S_h, mm (in.)	ρ_g, %	ρ_w, %	f_{syx}, MPa (ksi)	f_{syy}, MPa (ksi)	f_c', MPa (ksi)	P, kN (kips)	Failure mode
No. 12[6]	DC	300 (11.8)	300 (11.8)	900 (35.4)	150 (5.9)	2.26	0.14	415 (60)	410 (59)	28 (4.1)	540 (121)	1
No. 14[6]	DC	300 (11.8)	300 (11.8)	900 (35.4)	50 (2.0)	2.26	0.4	415 (60)	410 (59)	26 (3.8)	540 (121)	2
No. 15[6]	DC	300 (11.8)	300 (11.8)	900 (35.4)	50 (2.0)	2.26	0.85	415 (60)	410 (59)	26 (3.8)	540 (121)	2
No. 16[6]	DC	300 (11.8)	300 (11.8)	600 (23.6)	50 (2.0)	1.8	0.43	450 (65)	410 (59)	27 (3.9)	540 (121)	2
A1[7]	DC	150 (5.9)	420 (16.5)	1260 (49.6)	200 (7.9)	0.9	0.13	350 (51)	290 (42)	18.3 (2.7)	328 (74)	1
B1[7]	DC	300 (11.8)	300 (11.8)	900 (35.4)	160 (6.3)	1.69	0.08	336 (49)	290 (42)	18.3 (2.7)	477 (107)	1
2CLH18[8]	DC	457 (18)	457 (18)	2946 (116)	457 (18)	2	0.1	330 (48)	400 (58)	33 (4.8)	500 (112)	2
3CLH18[8]	DC	457 (18)	457 (18)	2946 (116)	457 (18)	3	0.1	330 (48)	400 (58)	25.6 (3.7)	500 (112)	1
No. 2[9]	DC	457 (18)	457 (18)	2946 (116)	305 (12)	2.5	0.17	434 (63)	476 (69)	21.1 (3.1)	2650 (596)	3
No. 4[9]	DC	457 (18)	457 (18)	2946 (116)	305 (12)	2.5	0.17	447 (65)	469 (68)	21.8 (3.1)	667 (150)	2
N18M[10]	DC	300 (11.8)	300 (11.8)	900 (35.4)	100 (3.9)	2.7	0.19	380 (55)	375 (54)	26.5 (3.8)	429 (96)	1
No. 1[11]	DC	200 (7.9)	400 (15.7)	1000 (39)	128 (5)	2.53	1	360 (52)	345 (50)	45 (6.5)	0	2
C5-00S[12]	SC	203 (8)	203 (8)	1220 (48)	76.2 (3)	1.93	1	573 (83)	515 (75)	37.9 (5.5)	0	3
C10-05S[12]	SC	203 (8)	203 (8)	1220 (48)	76.2 (3)	1.93	1	586 (85)	407 (59)	69.6 (10)	142 (32)	3
C10-10S[12]	SC	203 (8)	203 (8)	1220 (48)	76.2 (3)	1.93	1	574 (83)	515 (75)	67.8 (9.8)	285 (64)	3
C10-20N[12]	SC	203 (8)	203 (8)	1220 (48)	76.2 (3)	1.93	1	572 (83)	514 (75)	65 (9.4)	569 (128)	3
No. 4[13]	DC	400 (15.7)	400 (15.7)	3200 (126)	80 (3.1)	1.57	1.1	474 (69)	333 (48)	25.6 (3.7)	819 (184)	3
No.7 [13]	SC	550 (21.6)	550 (21.6)	3300 (130)	90 (3.5)	1.25	1	511 (74)	325 (47)	32.1 (4.6)	2913 (655)	3
B2[14]	DC	250 (9.8)	250 (9.8)	1000 (39.4)	40 (1.6)	2.43	0.4	379 (55)	774 (112)	99.5 (14.4)	2176 (449)	3
D1N3[15]	SC	242 (9.5)	242 (9.5)	1250 (49.2)	40 (1.6)	2.43	0.8	461 (67)	486 (71)	37.6 (5.5)	705 (158)	3
D1N6[15]	SC	242 (9.5)	242 (9.5)	1250 (49.2)	40 (1.6)	2.43	0.8	461 (67)	486 (71)	37.6 (5.5)	1410 (317)	3

Note: DC = double curvature or with two fixed ends; SC = single curvature or cantilever; b = width of section; h = depth of section; L_{in} = length of column from inflection point to end section; S_h = hoop spacing; ρ_g = longitudinal reinforcement ratio; ρ_w = transverse reinforcement ratio; f_{syx} = longitudinal reinforcement yield stress; f_{syy} = transverse reinforcement yield stress; f_c' = concrete compression strength; P = axial load; Failure Mode 1 = shear failure at crack $\varepsilon_2 < \varepsilon_c'$; Failure Mode 2 = loss of compression strength $\varepsilon_2 < \varepsilon_c'$; and Failure Mode 3 = shear-compression failure $\varepsilon_2 = \varepsilon_c'$.

$$\varepsilon_2 = \frac{\varepsilon_c + \varepsilon_{xa}}{2} \quad (29)$$

$$\varepsilon_x = \frac{\varepsilon_o + \varepsilon_{xa}}{2} \quad (30)$$

5. Using Eq. (13) through (15), determine ε_1 and ε_y. Because the problem is being solved for conditions at the ultimate state, usually the transverse reinforcement has yielded and only Eq. (15) need be applied;

6. Employ Eq. (12) to obtain $\tan\theta_c$;

7. Using Eq. (26) through (28), check for shear failure. If no failure has occurred, then increase ε_c and repeat the previous steps. If, for example, Eq. (26) shows shear failure at the crack, then ε_c must be reduced until all three equations provide greater or equal values;

8. Check for crushing of the cover concrete. This is not a failure model, but the axial load capacity will decline; strain hardening sometimes will help mitigate the decline. Check for buckling of the compression bars, bond failure, rupture of tensile bars, and compression softening factor $\beta \geq 0.15$;

9. Determine the ultimate deformation using Eq. (1), where

$$\gamma_f = \frac{\delta}{L_{in}} = \frac{1}{L_{in}} \int_0^{L_{in}} x\phi dx$$

and

$$\gamma_s = \frac{2(\varepsilon_x - \varepsilon_2)}{\tan\theta_c}$$

10. Finally, the ultimate lateral load capacity is obtained by

$$V_u = \tau_f bh \quad (31)$$

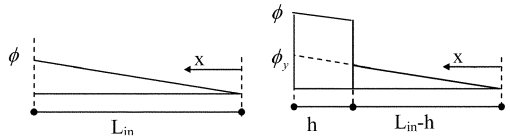

(a) Up to yield point of tensile steel (b) After yield point of tensile steel

Fig. 9—Presumed curvature distribution for reinforced concrete column.

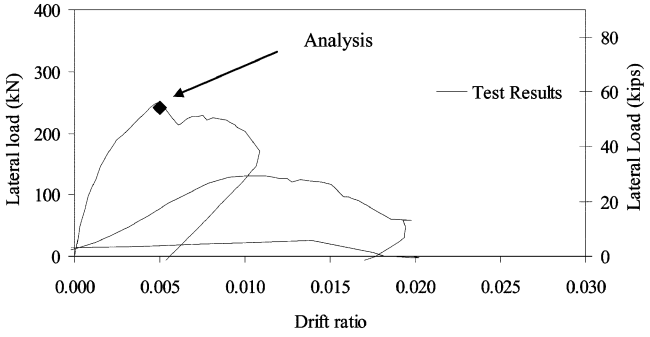

Fig. 10—Comparison of experimental result for Specimen 12 and ultimate deformation and load obtained from analytical model.

If the column or beam has sufficient transverse reinforcement, then the initial value for ε_c can be selected as $\varepsilon_c = 2\varepsilon_c' - \varepsilon_{xa}$, which is the limit for Failure Mode 3. Then check for other failure modes. If this is the dominant failure mode, then determine the ultimate drift.

Confinement effects can be taken into account for both shear and flexure models based on equations provided by Park et al.[2] Note that both the confinement factor and the compression softening factor, β, are applied in the constitutive law of compression concrete of the shear model. For the flexure model, however, only the confinement factor is considered and employed in the concrete stress-strain relationship.

NUMERICAL EXAMPLES

The analytical procedure was employed for Specimen 12, described in Table 1, with a shear-dominant response.

1. As an initial value, assume $\varepsilon_c = -0.002$.

2. To satisfy Eq. (23), an iteration procedure can be applied with few steps. First consider $\varepsilon_o = 0.002$ and $a = 0.85c$; hence

$$a = \frac{h\varepsilon_c}{(2.353\varepsilon_c - 1.353\varepsilon_o)}$$

or

$$a = \frac{300 \times (-0.002)}{2.353(-0.002) - 1.353(0.002)} = 81 \text{ mm (3.19 in.)}$$

From Eq. (22), $\varepsilon_s = 0.006$ and $\varepsilon_s' = -0.002$; thus Eq. (23) gives $\varepsilon_o = 0.00265$. After three or four iterations, ε_o converges to 0.00296.

3. The axial strain at the inflection point with zero moment can be determined as

$$\varepsilon_{xa} = \frac{(P/bh)}{(2f_p/\varepsilon_p + E_s\rho_{sx})} = -0.00019$$

where $2f_p/\varepsilon_p$ is the average concrete modulus of elasticity of section at the inflection point and ε_p and f_p are confined concrete peak strain and stress, respectively, which are determined based the confinement model by Park et al.[2] For simplicity, they might be considered equal to ε_c' and f_c', respectively.

4. The average concrete principal compression strain ε_2 and axial strain ε_x for the shear model are then obtained by

$$\varepsilon_2 = \frac{\varepsilon_c + \varepsilon_{xa}}{2} = -0.00101$$

and

$$\varepsilon_x = \frac{\varepsilon_o + \varepsilon_{xa}}{2} = 0.0014$$

5. Assuming yielding of the transverse bars, Eq. (15) can be employed to obtain ε_1

$$\varepsilon_1 = \frac{(\varepsilon_x - \varepsilon_2)(f_{c1} - \sigma_x + \rho_{sx}E_s\varepsilon_x)}{(f_{c1} + \rho_{sy}f_{syy})} + \varepsilon_x$$

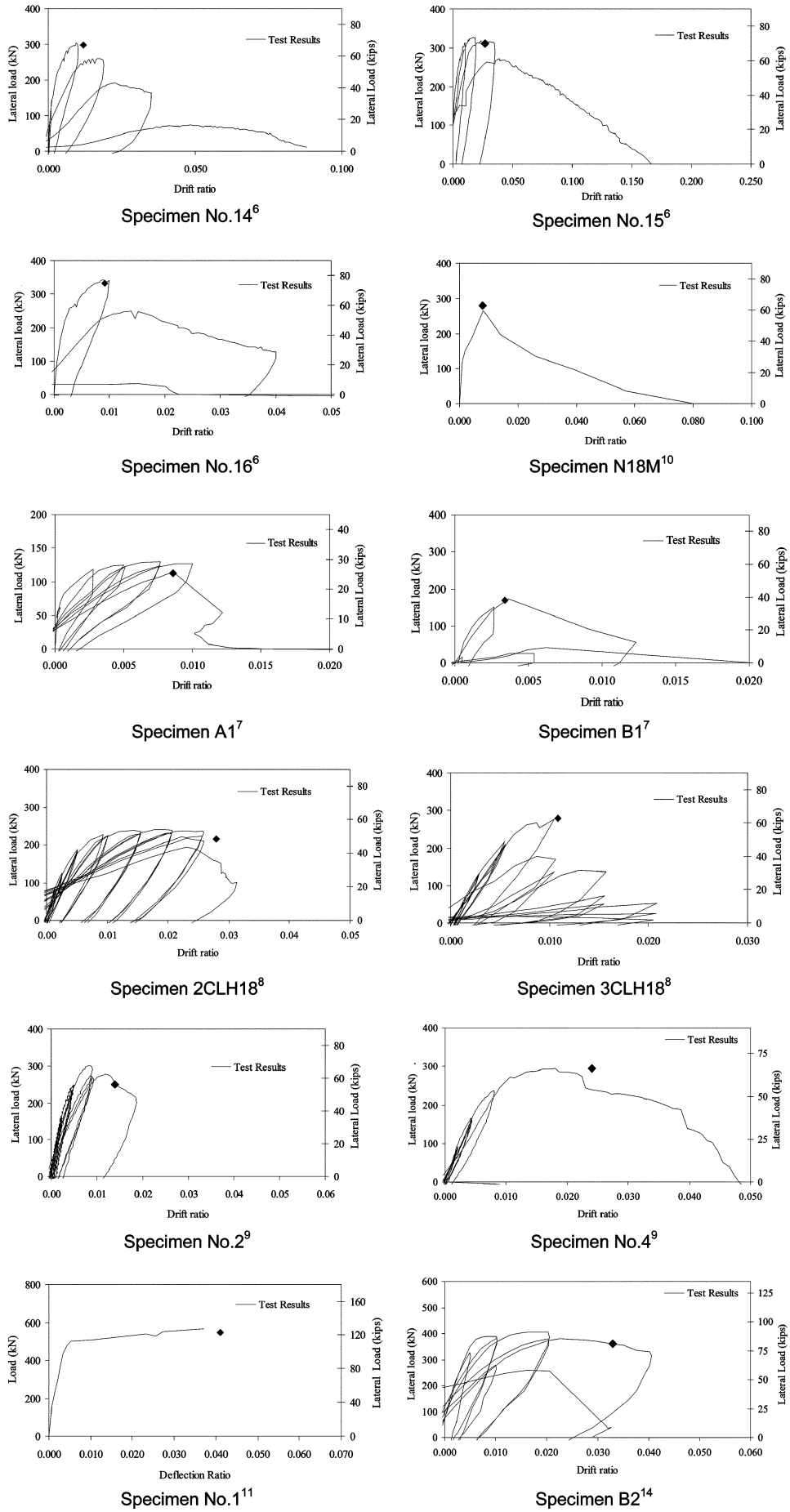

Fig. 11—Comparison of experimental and analytical results. (Continued on next page.)

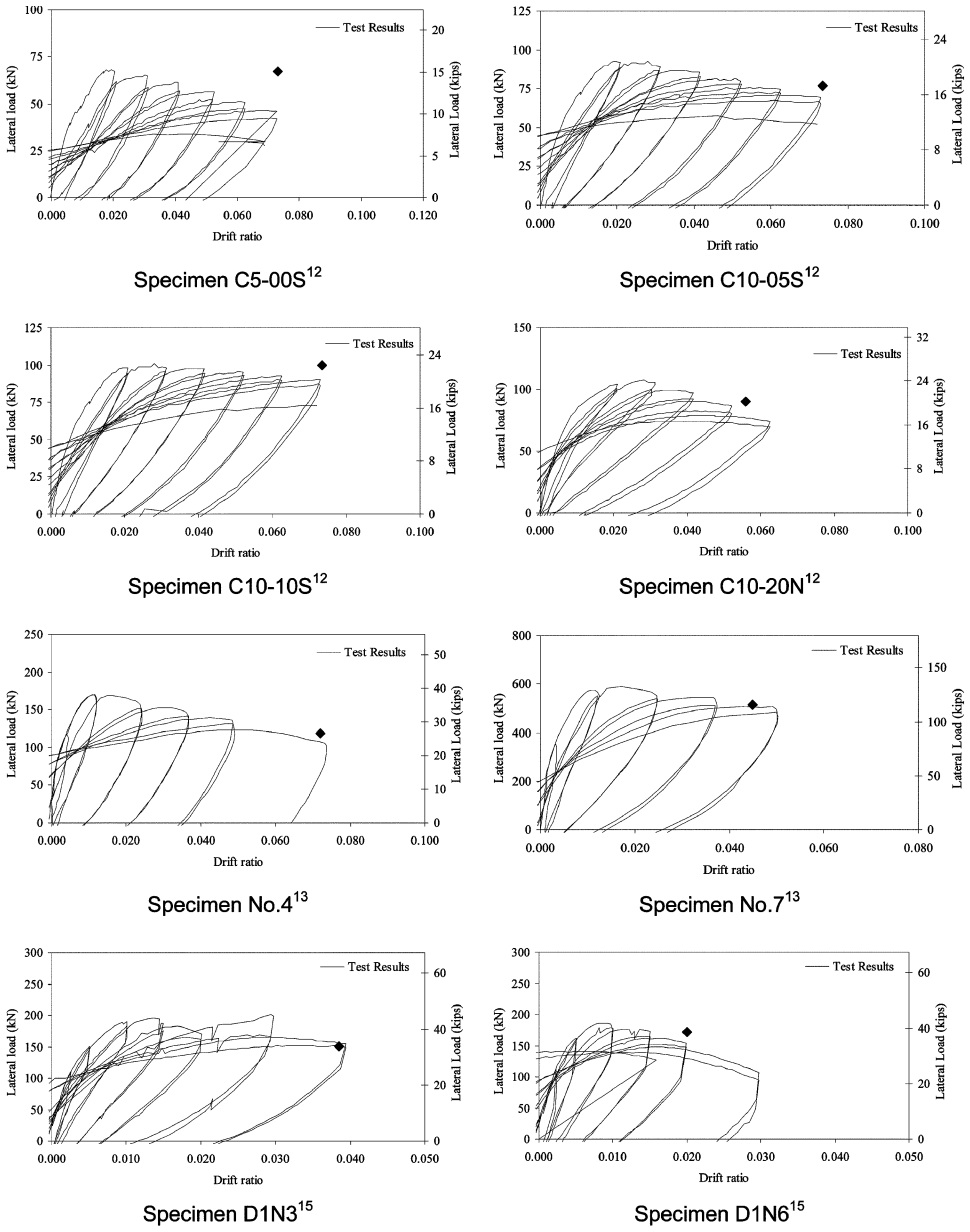

Fig. 11 (cont'd)—Comparison of experimental and analytical results.

where $\sigma_x = \sigma_o = P/bh$, $f_{c1} = 0.44f_v' = 0.44 \times 0.33\sqrt{f_c'} = 0.44 \times 0.33\sqrt{28} = 0.77$ MPa (111.7 psi); hence, $\varepsilon_1 = 0.024$.

6. Equation (12) is employed, producing the result of $\tan\theta_c = 0.33$.

7. Checking for shear failure at a crack using Eq. (26), the moment is obtained by Eq. (24).

$$\frac{M}{bdL_{in}} = \frac{1.26\times10^8}{300 \times 260 \times 450} =$$

$$3.59 \geq \tau_i + f_{syy}\rho_{sy}\cot\theta = 2.17$$

where τ_i is computed using Eq. (17).

The result indicates that a shear failure at crack has occurred, hence ε_c must be reduced.

Selecting $\varepsilon_c = -0.001$ and repeating the previous steps results in

$$\tau_f = \frac{M}{bhL_{in}} =$$

$$2.89 \cong \tau_i + f_{syy}\rho_{sy}\cot\theta_c = 2.97 \text{ MPa (430.76 psi)}$$

Therefore, shear failure at a crack (that is, Failure Mode 1) is defined as the governing failure mechanism of this specimen at the ultimate state.

8. From the test, there is no sign of cover concrete crushing or other failure criteria governing. Usually, Mode 1 failure gives the lowest ultimate drift ratio.

9. Based on the curvature distribution shown in Fig. 9, the shear and flexural deformations are determined

$$\gamma_f = \frac{\delta}{L_{in}} = \frac{1}{L_{in}}\int_0^{L_{in}} x\phi dx = 0.002 \text{ and}$$

$$\gamma_s = \frac{2(\varepsilon_x - \varepsilon_2)}{\tan\theta_c} = 0.0029$$

$$\gamma = \gamma_f + \gamma_s = 0.0049$$

10. Finally, calculation of the ultimate lateral load capacity results in $V_u = \tau_f bh = 260$ kN (58 kips).

The ultimate load and deformation obtained for this sample problem are compared in Fig. 10 to the experimental result, exhibiting good correlation. A photograph of the specimen at the ultimate state is shown in Fig. 8, depicting a pronounced shear failure on the face of the column. As a second example, the ultimate deformation and load are determined for Specimen 16 in Table 1.

The iteration for this example results in $\varepsilon_c = -0.00135$ with Mode 2 governing, where

$$\tau_f = \frac{M}{bhL_{in}} =$$

$$4.05 \cong \frac{(f_{c1} - f_{c2})}{(\tan\theta_c + 1/\tan\theta_c)} = 4.17 \text{ MPa (604.81 psi)}$$

while the other failure conditions are satisfied. As a result, the ultimate deformation is determined as: $\gamma = \gamma_f + \gamma_s = 0.009$ with a lateral force of $V_u = \tau_f bh = 364$ kN (82 kips), both values nearly perfectly correlated to the experimental result, as seen in Fig. 11. Note that few iterations are required for Step 2 of the analytical procedure. For all the column specimens studied in this investigation, only two or three iterations were required to achieve convergence. To avoid the iteration process, it is also possible to solve Eq. (23) by deriving different equations dependent only on the yield states of the compressive and tensile bars. However, the authors found Eq. (23) more efficient to apply as a general equation and applicable for all the stress-strain conditions.

The ultimate deformation estimation approach was employed for all specimens in Table 1. Comparisons between the experimental and analysis are plotted in Fig. 11, indicating consistently accurate correlations. Because the shear capacity, obtained from the analysis, is based on the section moment capacity without consideration of geometrical nonlinearity, the P-Δ effect due to drift is determined and employed for the flexural columns, which reduces the calculated shear capacity. Failure modes are determined and given in Table 1 for all the reinforced concrete columns specimens.

CONCLUSIONS

An analytical approach was developed to estimate the ultimate deformation and load capacity of reinforced concrete columns based on a simplified axial-shear-flexure interaction approach. Shear failure was the main failure criteria for both flexure- and shear-dominant specimens. In this approach, the concrete compression softening factor was employed only within the MCFT-based shear model. Axial strain and concrete compression strain were the two main parameters common to both the shear and axial models. Three failure modes were defined as the main ultimate state conditions: shear failure at the cracks, loss of concrete compression strength before the peak, and finally shear-compression failure when $\varepsilon_2 = \varepsilon_c'$. The ultimate deformation and load capacity results obtained by the new approach were verified against experimental data; consistent correlations between the analytical and experimental results for a series of reinforced concrete columns were attained.

REFERENCES

1. Elwood, K. J., and Moehle, J. P., "Drift Capacity of Reinforced Concrete Columns with Light Transverse Reinforcement," *Earthquake Spectra*, Earthquake Engineering Research Institute, V. 21, Feb. 2005, pp. 71-89.

2. Park, R.; Priestley, M. J. N.; and Gill, W. D., "Ductility of Square Confined Concrete Columns," *Journal of Structural Division*, ASCE, V. 108, No. 4, 1982, pp. 929-950.

3. Mostafaei, H., and Kabeyasawa, T., "Axial-Shear-Flexure Interaction Approach for Reinforced Concrete Columns," *ACI Structural Journal*, V. 104, No. 2, Mar.-Apr. 2007, pp. 218-226.

4. Mostafaei, H., "Axial-Shear-Flexure Interaction Approach for Displacement-Based Evaluation of Reinforced Concrete Elements," PhD dissertation, Faculty of Engineering, Architrave Department, University of Tokyo, Tokyo, Japan, 2006, 255 pp.

5. Vecchio, F. J., and Collins, M. P., "The Modified Compression Field Theory for Reinforced Concrete Elements Subjected to Shear," ACI Journal, *Proceedings* V. 83, No. 2, Mar.-Apr. 1986, pp. 219-231.

6. Ousalem, H.; Kabeyasawa, T.; Tasai, A.; and Iwamoto, J., "Effect of Hysteretic Reversals on Lateral and Axial Capacities of Reinforced Concrete Columns," *Proceedings of the Japan Concrete Institute*, V. 25, No. 2, 2003, pp. 367-372.

7. Koizumi, H., "A Study on a New Method of Sheet Strengthening to Prevent Axial Collapse of RC Columns during Earthquakes," master's thesis, Faculty of Engineering, Architrave Department, University of Tokyo, Toyko, Japan, 2000, 94 pp. (in Japanese)

8. Lynn, A. C.; Moehle, J. P.; Mahin, S. A.; and Holmes, W. T., "Seismic Evaluation of Existing Reinforced Concrete Building Columns," *Earthquake Spectra*, V. 12, No. 4, 1996, pp. 715-739.

9. Sezen, H., "Evaluation and Testing of Existing Reinforced Concrete Columns," *CE 299 Report*, Department of Civil and Environmental Engineering, University of California-Berkeley, Berkeley, CA, 2000, 324 pp.

10. Nakamura, T., and Yoshimura, M., "Gravity Collapse of Reinforced Concrete Columns with Brittle Failure Modes," *Journal of Asian Architecture and Building Engineering*, V. 1, No. 1, 2002, pp. 21-27.

11. Umemura, H.; Aoyama, H.; and Noguchi, H., "Experimental Studies on Reinforced Concrete Members and Composite Steel and Reinforced Concrete Members," V. 2, Faculty of Engineering, Department of Architecture, University of Tokyo, Tokyo, Japan, 1977, pp. 113-130.

12. Matamoros, A. B., "Study of Drift Limits for High-Strength Concrete Columns," Department of Civil Engineering, University of Illinois at Urbana-Champaign, Urbana, IL, Oct. 1999.

13. Tanaka, H., and Park, R., "Effect of Lateral Confining Reinforcement on the Ductile Behavior of Reinforced Concrete Columns," *Report* 90-2, Department of Civil Engineering, University of Canterbury, Christchurch, New Zealand, June 1990, 458 pp.

14. Sakai, Y.; Hibi, J.; Otani, S.; and Aoyama, H., "Experimental Study on Flexural Behavior of Reinforced Concrete Columns Using High-Strength Concrete," *Transactions of the Japan Concrete Institute*, V. 12, 1990, pp. 323-330.

15. Kono, S., and Watanabe, F., "Damage Evaluation of Reinforced Concrete Columns under Multiaxial Cyclic Loadings," The Second U.S.-Japan Workshop on Performance-Based Earthquake Engineering Methodology for Reinforced Concrete Building Structures, 2000, pp. 221-231.